ERDC TR-14-6

US Army Corps
of Engineers®
Engineer Research and
Development Center

ERDC
ENGINEER RESEARCH & DEVELOPMENT CENTER

Materials Modeling for Force Protection

Development of the Particle-Scale Definition of Stress and Strain for the Discrete Element Method

Report 3 in "Discrete Nano-Scale Mechanics and Simulations" Series

W. D. Hodo, J. F. Peters, L. E. Walizer, D. P. McInnis,
and A. R. Carrillo

April 2019

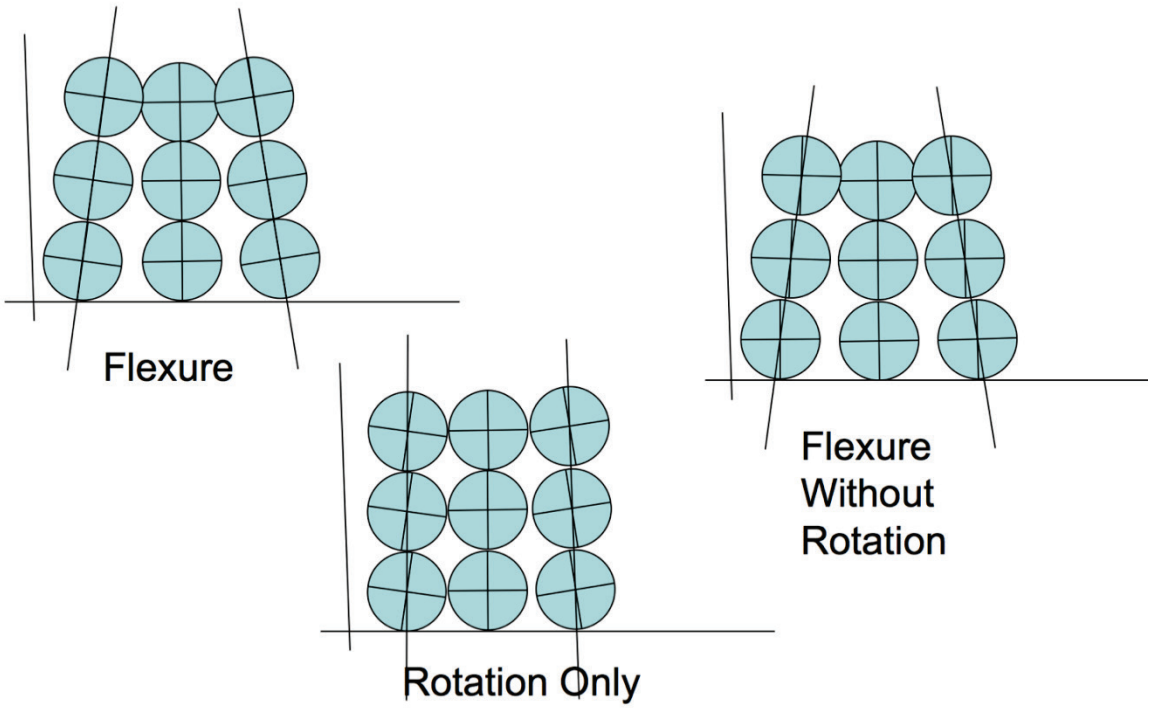

Engineer Research and
Development Center

The U.S. Army Engineer Research and Development Center (ERDC) solves the nation's toughest engineering and environmental challenges. ERDC develops innovative solutions in civil and military engineering, geospatial sciences, water resources, and environmental sciences for the Army, the Department of Defense, civilian agencies, and our nation's public good. Find out more at www.erdc.usace.army.mil.

To search for other technical reports published by ERDC, visit the ERDC online library at http://acwc.sdp.sirsi.net/client/default.

ERDC TR-14-6
April 2019

Development of the Particle-Scale Definition of Stress and Strain for the Discrete Element Method

Report 3 in "Discrete Nano-Scale Mechanics and Simulations" Series

W. D. Hodo, J. F. Peters (Retired), L. E. Walizer, and D. P. McInnis

Geotechnical and Structures Laboratory
U.S. Army Engineer Research and Development Center
3909 Halls Ferry Road
Vicksburg, MS 39180-6199

A. R. Carrillo

Coastal and Hydraulics Laboratory
U.S. Army Engineer Research and Development Center
3909 Halls Ferry Road
Vicksburg, MS 39180-6199

Report 3 of a series

Supersedes ERDC/CERL AF-01-23

Prepared for U.S. Army Corps of Engineers
Washington, DC 20314-1000

Under Military Engineering AT22/AT40 program, Materials Modeling for Force Protection," Work Units #PM001 and #MR001: Discrete Nano-Scale Mechanics and Simulations

Abstract

The discrete element method (DEM) provides a realistic approach to modeling materials at fundamental length scales. Materials at the *discrete scale* can be the particle size in granular materials, micrometer sizes when dealing with polycrystalline materials, or nanometer sizes when dealing with biologic materials. Complex material behavior can be simulated as relatively simple interactions between discrete entities, obviating the need for sophisticated constitutive models. The ultimate goal is to obtain the engineering behavior at the prototype scale at which problems are formulated in terms of continuum mechanics.

The simple concepts of kinematics for the discrete entities are tied to continuum quantities using affine projections and thermodynamic conjugates. The continuum quantities such as force and displacement are equated to their continuum counterparts, stress and strain, using the method of virtual power. The kinematics at the fundamental scale include the rotations of the discrete elements, which in contrast to those of material points in a continuum are independent of the translational motion. To accommodate the rotations as independent variables, the Cosserat continuum theory is used.

The procedures are implemented in a Fortran subroutine, which can be used in the post-processing phase of DEM simulations. Example computations for three test cases are included.

Contents

Figures and Tables

Figures

Tables

Preface

This study was conducted for the U.S. Army Engineer Research and Development Center (ERDC) under the Military Engineering Work Units #PM001 and #MR001 "Discrete Nano-Scale Mechanics and Simulations."

The study was conducted by the Airfields and Pavements Branch (GMA), Impact and Explosion Effects Branch (GMI), and Mobility Systems Branch (GMM) of the Engineering Systems and Materials Division (GM), ERDC Geotechnical and Structures Laboratory (ERDC-GSL) and the Estuarine Engineering Branch (HFE) of the Flood & Storm Protection (HF) Division, ERDC Coastal and Hydraulics Laboratory (ERDC-CHL). At the time of publication, Dr. Timothy W. Rushing was Chief, CEERD-GMA; Mr. Jeffery G. Averett was Chief, CEERD-GMI; Mr. Jeff Durst was Chief, CEERD-GMM; Mr. Robert T. McAdory was Chief, CEERD-HFE; Mr. Justin Strickler was Acting Chief, CEERD-GM; Mr. Hwai P. Cheng was Acting Chief, CEERD-HF; and Ms. Pamela G. Kinnebrew, CEERD-GZT, was Technical Director for Military Engineering. The Deputy Director for ERDC-GSL was Mr. Charles W. Ertle II, and the Director was Mr. Bartley P. Durst. The Deputy Director for ERDC-CHL was Mr. Jeffrey R. Eckstein and the Director was Dr. Ty V. Wamsley.

COL Ivan P. Beckman was the Commander of ERDC, and Dr. David W. Pittman was the Director.

Unit Conversion Factors

Multiply	By	To Obtain
cubic feet (ft^3)	0.02831685	cubic meters
cubic inches ($in.^3$)	1.6387064 E-05	cubic meters
feet (ft)	0.3048	meters
inches (in.)	0.0254	meters
inch-pounds (force)	0.1129848	newton meters
pounds (force) (lb)	4.448222	newtons
pounds (force) per square foot ($lb/ft^{2)}$	47.88026	pascals
pounds (force) per square inch ($lb/in.^2$)	6.894757	kilopascals
pounds (mass) (lb)	0.45359237	kilograms
pounds (mass) per cubic foot (lb/ft^3)	16.01846	kilograms per cubic meter
pounds (mass) per cubic inch ($lb/in.^3$)	2.757990 E+04	kilograms per cubic meter
pounds (mass) per square foot (lb/ft^2)	4.882428	kilograms per square meter
square feet (ft^2)	0.09290304	square meters
square inches ($in.^2$)	6.4516 E-04	square meters

1 Introduction

The discrete element method (DEM) provides a realistic approach to modeling materials at length scales where the mechanics can be formulated as interactions among discrete components. The *discrete scale* can be the particle size in granular materials such as sand, micrometer sizes when dealing with polycrystalline materials, or nanometer sizes when dealing with biologic materials. However, in all cases, the ultimate goal is to obtain the engineering behavior at a *prototype scale* at which computations are to be performed. For prototype scale computations, phenomenological constitutive equations are used to define the mechanical response. Such relationships are derived from experiments on macro engineering scale (continuum level) specimens. The continuum level assumes that effects of discrete scale processes are observed in an average sense in the form of processes described as elastic, plastic, viscoelastic/plastic, damage, and so on. Such descriptions are based on characteristics of the stress-strain response with no direct observations of the fundamental processes causing the response. Often, it is difficult to make observations of materials at smaller scales, even in posttest analyses, much less during loading. By contrast, simulations offer quantitative data, at all stages of loading, on motions and forces associated with the deforming discrete media. Moreover, properties used to calibrate the models tend to have a closer relationship to fundamental processes and often involve fewer numerical parameters. The reason for the parsimony of parameters comes from the large role that discrete kinematics play in the response at the more fundamental scale. Given accurate simulation models, the question to be asked is how are the discrete processes at the small scale to be related to the engineering parameters used to describe the large scale?

The effort to apply micro-scale quantities to macro-scale (continuum) theories ultimately revolves around the definitions of stress and strain. When attempting to apply continuum theories of discrete media, such definitions reflect an averaging process that relates the particle quantities within a sampling volume to a macro-scale quantity assigned to the volume. For a continuum theory, that volume average must apply to infinitesimal volumes based on the invariance of the governing laws to the volume size. Thus, there is at some level of resolution an inability for the continuum model to capture important details of granular behavior. As a

practical matter, such discrepancies can be overlooked except in cases where scale-dependency arises, notably cases of shear localization and wave dispersion.

1.1 Objective

The objective of this report is to present an approach to averaging discrete-scale processes to obtain the engineering-scale continuum properties at the larger scale. This averaging procedure addresses the problem of relating discontinuous processes at the discrete scale to the continuous processes assumed in continuum models as well as the issues of what constitutes a suitable average. The second of these issues is largely statistical whereas the first issue is more fundamental; for it is the discontinuous behavior that gives rise to much of the non-elastic phenomena described by continuum constitutive equations.

1.2 Goals and summary of report

In the remainder of the report a method is proposed to extract from DEM simulations work-consistent relationships for stress, stress couples, strain, and rotations. Chapter 2 introduces the basic concepts. In Chapter 3, the extraction of kinematic quantities is addressed by the concept of projecting continuum motions to the particle system, which provides correlations between continuum and discrete kinematics. It was easily demonstrated that generalized stresses and couples can be derived using the virtual power method. This tact is followed in Chapter 4 where the specific relationships for a Cosserat continuum are derived. Chapter 5 presents a specific example of data extraction from a DEM simulation. Conclusions and recommendations for future research are in Chapter 6.

2 Basic Concepts

The analysis in this report involves two issues. First, there is the relationship between the idealized continuum and the discrete element system. The continuum motion of granular media is an emergent behavior that characterizes the average particle velocities. Therefore, in all measurements, a sampling volume must be assigned. In view of the finite nature of the particle sizes, the sampling volume must be a *Representative Element Volume* (REV), which is sufficiently large to define a stable average. In continuum derivations, it is assumed that the elemental volume is arbitrary and includes arbitrarily small (infinitesimal) volumes. The finite size of the sampling volume introduces a non-locality to the theory and admits rotations as an independent kinematic variable. The motion is also heterogeneous giving rise to so-called non-affine motions of the particles. Such motions give rise to dissipative processes such as plasticity and damage.

The second issue is the boundary condition for the sampling volume. The procedure presented in this report avoids defining a condition at the sample boundary by instead imposing a condition on the average behavior, denoted the projected motion, which by definition is an affine motion. The stress quantities are defined as the thermodynamic conjugates to the affine motions. For static equilibrium, only the particles on the boundary of the REV are non-zero, thus the stress is defined in terms of boundary forces. A discussion of the "stress" quantities conjugate to the non-affine motions is included in Section 3.2.1.

2.1 Notation

The granular medium consists of N^p particles interacting though N^c contacts. The number of contacts that a particular particle p makes with its immediate neighbors is denoted by M^p. A contact c consists of an interaction between two particles denoted A and B. Accordingly, the contribution of a contact quantity from particle A is denoted by the superscript A_c and for particle B as B_c. The A and B represent the arbitrarily assigned particle numbers, and the subscript c denotes contact quantities.

Index notation is used to present vector and tensor quantities. Indices are presented as subscripts whereas particle and contact numbers are indicated as superscripts. For example, the vector connecting the center of

particle A to the contact c would be denoted $r_i^{A_c}$; the radius connecting to the contact from the B particle would be $r_i^{B_c}$. The contact force and moment are denoted as f_i^c and m_i^c, respectively, because they are shared by two particles. By convention, the contact force and moment directions are positive when viewed from particle A. If these quantities are to be associated with the particles on which they act, the nomenclature would be $f_i^{A_c}$, $f_i^{B_c}$, $m_i^{A_c}$, and $m_i^{B_c}$, in which case their directions would take on the sign consistent with the particles on which they act.

The contact number can either refer to the global system of contacts or to the contacts associated with a particular particle. A convenient device used in the analysis is expressing double summations of particles and their contacts as single summations over the global contacts (see next Section 2.2). Whether c is used to denote a global number or a contact local to a particular particle can be determined from the context in which the expression is used. In addition to standard tensor notation, in Section 3.1 a matrix notation is introduced to facilitate the least-square procedure for determining strain and rotation. The correspondence between the tensor and matrix representations is also given in Section 3.1.

2.2 Contact averages

Average quantities for the discrete media are computed from summations taken over particles and/or contacts. An example of a sum of some particle quantity Q would be

$$\sum_{p \in N^p} Q^p$$

The range of the summation is given by the common nomenclature $p \epsilon N^p$, which defines the summation index and range. The present example is a summation of the quantity Q for the total population of N^p particles, with the index p ranging over each particle in the population. For the case of a quantity Q defined at a contact of a particle, the summation would be computed as a partial summation over the contacts of the particle, which is then summed over the population of particles, *vis*

$$\sum_{p \in N^p} \sum_{c \in M^p} Q^c.$$

Recall that M^p is the number of contacts for particle p. Such summations can be replaced with sums over the population of contacts by recognizing that each quantity for contact c is made up of particle pairs denoted A_c and B_c. Summations over contact quantities satisfies the following relationship for some quantity Q^{p_c} defined as the quantities Q in particle p at each particle contact c

$$\sum_{\boldsymbol{p\in N^p}} \sum_{\boldsymbol{c\in M^p}} \boldsymbol{Q^c} = \sum_{\boldsymbol{p\in N^c}} (\boldsymbol{Q^{A_c}} + \boldsymbol{Q^{B_c}}). \tag{1}$$

Further, each contact force must satisfy the momentum balance $f_i^{A_c} = -f_i^{B_c}$, and each contact moment must satisfy $m_i^{A_c} = -m_i^{B_c}$. Thus, for example, it is readily seen that

$$\sum_{p\in N^p} \sum_{c\in M^p} f_i^c = 0 \tag{2}$$

wherein

$$\begin{aligned} \sum_{p\in N^p} \sum_{c\in M^p} f_i^c &= \sum_{c\in N^c} \left(f_i^{A_c} + f_i^{B_c}\right) \\ &= \sum_{c\in N^c} \left(f_i^{A_c} - f_i^{A_c}\right) \\ &= 0. \end{aligned}$$

2.3 Average stress

The starting point of the discussion is a review of the definition of mean stress within a continuum volume V bounded by surface S acted on by tractions t_i. The average stress within a continuum is defined as

$$\langle \sigma_{ij} \rangle = \frac{1}{V} \int_V \sigma_{ij} dV \tag{3}$$

where the stress, σ_{ij}, satisfies the momentum balance (in the absence of body forces)

$$\frac{\partial \sigma_{ij}}{\partial x_j} = 0, \tag{4}$$

and $\langle \sigma_{ij} \rangle$ signifies the volumetric average. Equation (4) is the equilibrium statement representing the sum of forces over index j in the i direction. For a virtual velocity δv_i, the virtual power on the infinitesimal element is given by

$$d(\delta P) = \frac{\partial \sigma_{ij}}{\partial x_j} \delta v_i dV.$$

The variation of velocity within the volume is defined by the strain as $\delta v_i = \delta \dot{\varepsilon}_{ij} x_j$, giving the virtual power to be

$$d(\delta P) = \frac{\partial \sigma_{ij}}{\partial x_j} \delta \dot{\varepsilon}_{ij} x_j dV.$$

Consider now the virtual power associated with a linear variation of virtual velocity $\delta v_i = \delta \dot{\varepsilon}_{ij} x_j$ for a stress field in equilibrium.

$$\delta P = \frac{1}{V} \int_V \frac{\partial \sigma_{ij}}{\partial x_j} \delta \dot{\varepsilon}_{jk} x_k dV. \tag{5}$$

In view of Equation (4), $\delta \mathrm{P} = 0$. Also, whereby the tensor $\delta \dot{\varepsilon}_{ij}$ is a constant, the power expression reduces to a weak form of the equilibrium equation

$$\frac{1}{V} \int_V \frac{\partial \sigma_{ij}}{\partial x_j} x_j dV = 0. \tag{6}$$

Applying the usual integral theorems to this expression — and in view of Cauchy's law, $t_i = \sigma_{ij} n_j$ — gives the average stress within a continuum body to be

$$\langle \sigma_{ij} \rangle = \frac{1}{V} \int_S t_j x_i dS, \tag{7}$$

where S is the surface of volume V. It follows that the average stress in a body is conjugate to a constant virtual strain rate that defines a linear

variation in virtual velocity. This velocity will be referred to as the projection of the virtual strain rate throughout the body.

2.4 Particle stress

The particle stress is defined as the average stress within each particle. The particle stress is approximated from Equation (7) by assuming the contact stresses can be represented as point forces f_i^c using delta operators, giving the usual formula*

$$\sigma_{ij}^p = \frac{1}{V_p}\sum_{c=1}^{N_c} r_i^c f_j^c. \tag{8}$$

For spherical particles, r_i^c is the radius vector directed from the particle center to the contact on the particle surface, which corresponds in direction to the normal vector for the particle surface at the point of contact.

2.5 The continuum stress

The average continuum stress is related to the average of the particle stress by noting that the stress within the void space is zero. Thus, from Equation (3) and with the assumption that the particle stress is independent of particle volume, the average stress for a volume of spherical particles becomes

$$\begin{aligned}\langle\sigma_{ij}\rangle &= \frac{1}{V}\sum_{p=1}^{N_p} V_p\sigma_{ij}^p \\ &= \frac{V_s}{V}\langle\sigma_{ij}^p\rangle\end{aligned} \tag{9}$$

where V_s is the total volume of solids within volume V and is equal to $\sum_{p \in N_p} V_p$. The ratio V_s/V is the fraction of the particle (solid) volume to the total volume. The solid fraction is denoted n_s and by definition is equal to $1-n$, where n is the porosity as traditionally used in geology and soil mechanics.

* This definition is equivalent to the viral stress under the temperature condition of absolute zero.

2.6 Example

An example computation of the particle stress and corresponding continuum stress will be presented. In that case, V is the volume of the REV. The micromechanical model is based on the Voronoi tessellation, shown in Figure 1, where each polygon becomes a portion of the REV. For the present discussion, an example will be used of a single particle within a square Voronoi cell of size $2R$ as shown in Figure 2. To illustrate the principle, it is sufficient to consider σ_{11}. For the case of two-dimensional particle systems, $V_p = \pi R^2$ giving the particle stress to be

$$\sigma_{ij}^{p} = \frac{1}{\pi R}\sum_{c=1}^{N_c} n_i^c f_j^c. \tag{10}$$

where n_i^c is the contact normal and Rn_i^c is r_i^c in Equation (8). The average stress in the continuum volume is $\langle\sigma_{11}\rangle = f_1/(2R)$. This is the stress that would be measured in an experiment. The particle stress is computed from Equation (10) as $\sigma_{11}^{p} = 2f_1/(\pi R)$. The ratio of the two stresses is $\langle\sigma_{11}\rangle/\sigma_{11}^{p} = \pi/4$. For comparison, the particle volume is πR^2 while the total volume is $4R^2$ to give $n_s = \pi/4$.

2.7 Particle rotations

For granular media, the definition of average stress is widely agreed upon; the definition of strain is not as well established. The problem that is still not fully resolved is the role of particle rotations. At the scale of the particles, the role of particle rotation is clearly defined by the particle kinematics. For the continuum, a theory that included rotations has been known since the work of the Cosserat brothers (Cosserat and Cosserat 1909) at the end of the 19th century and was later revived by Mindlin and Tiersten (1962) for micro-polar media and specifically for soils by Mühlhaus and Vardoulakis (1987). The relationship between the Cosserat theory and the rotations of the discrete particles is only partly resolved. In particular, the asymmetry of the stress that appears in

Figure 1. Particle sampling volume created by a Voronoi tessellation of a particle assemblage.

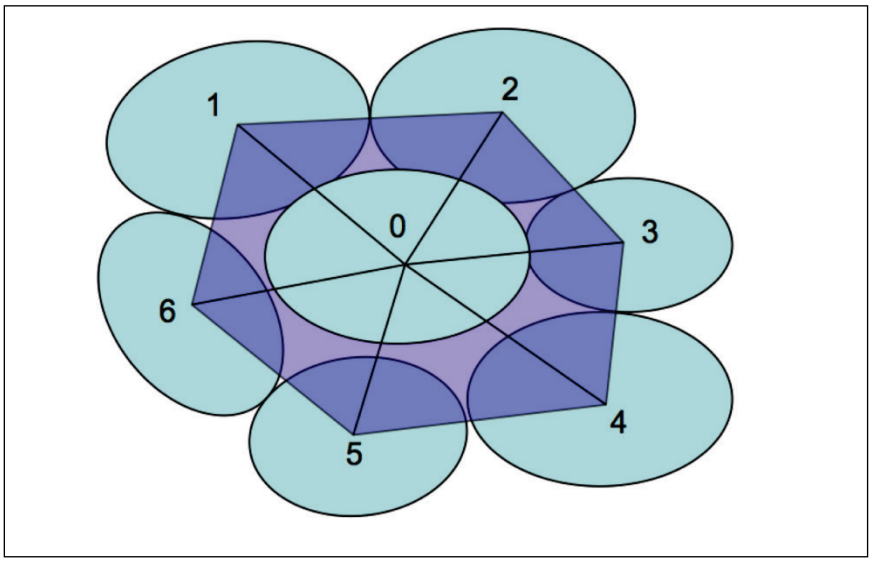

Figure 2. Particle within REV for example of stress computation.

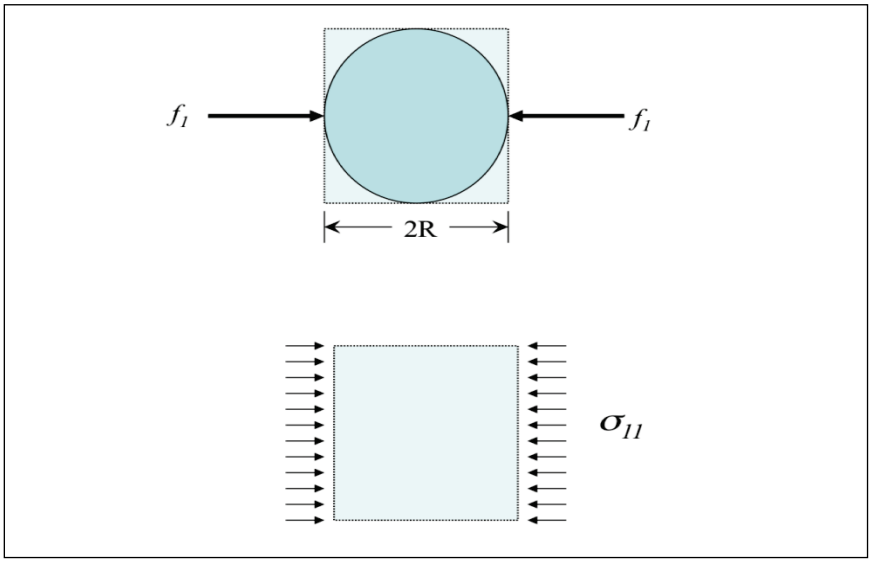

Cosserat media is still controversial (Bardet and Vardoulakis 2001). The application of the Cosserat theory in the analysis of stability in granular media is given in Sulem and Vardoulakis (2004). A mathematical review of the Cosserat theory for granular media that acknowledges many of the issues addressed in this report is given in Alonso-Marroquín (2011).

Rotation is an essential part of particle kinematics. The motion of contacts is the combined result of translation of particle centers and relative particle rotation (Figure 3). Figure 4 illustrates the interplay

between the translation of particle centers and motion at contacts. When the particle assemblage undergoes rigid-body rotation, the particles are uniformly rotating. However, the motion of particle centers offsets this rotation such that no contact movement occurs, no energy is stored or released, and no energy is dissipated. Thus, the uniform particle rotation is merely the result of the rigid-body rotation of the assemblage. But in a discrete medium there can be uniform particle rotation without rigid-body rotation. In the absence of rigid-body rotation of the assemblage, particle rotation causes contact motions, inducing tangential motion on the contact plane that imparts elastic energy or dissipates energy through contact sliding.

Figure 3. The kinematics of the particle pair that defines the contact. The relative translation, v_t^s, and rotation, ω_i, at the contact is the sum of contributions from relative particle translation, $v^A - v^B$ and rotation $\omega^A - \omega^B$.

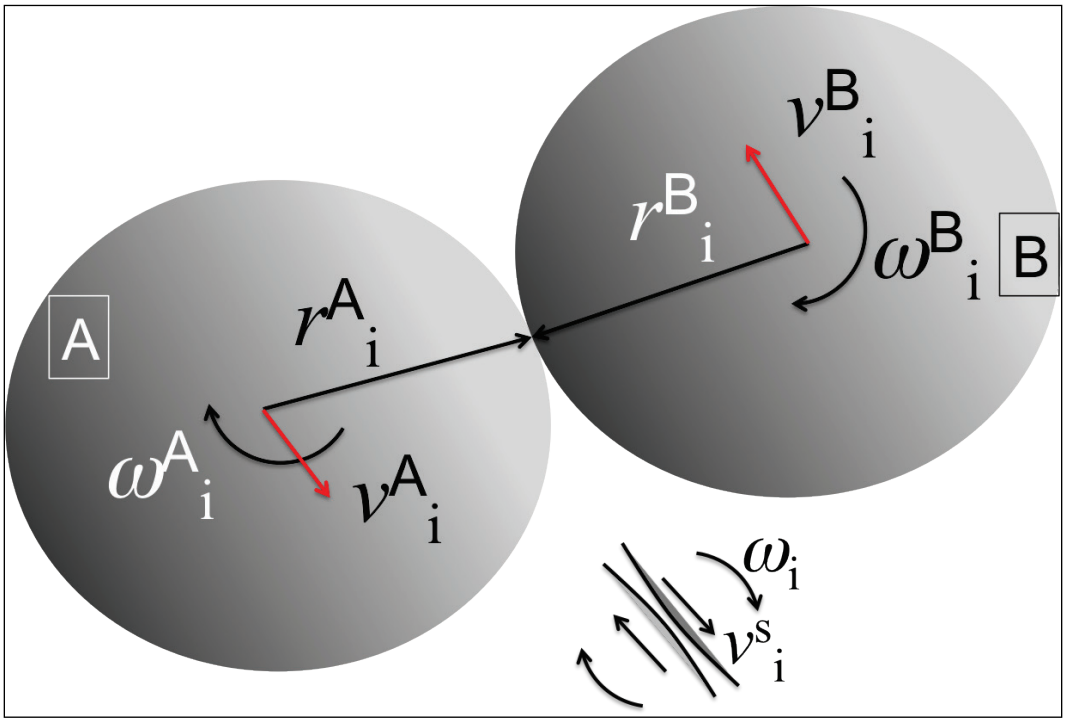

Figure 4. Particle rotations: (a) initial configuration of particles; (b) uniform rotations due to rigid-body rotation, $\omega_3{}^o$, which causes no contact dislocation; (c) uniform rotations ω_3, not caused by rigid-body rotation, which causes contact dislocations.

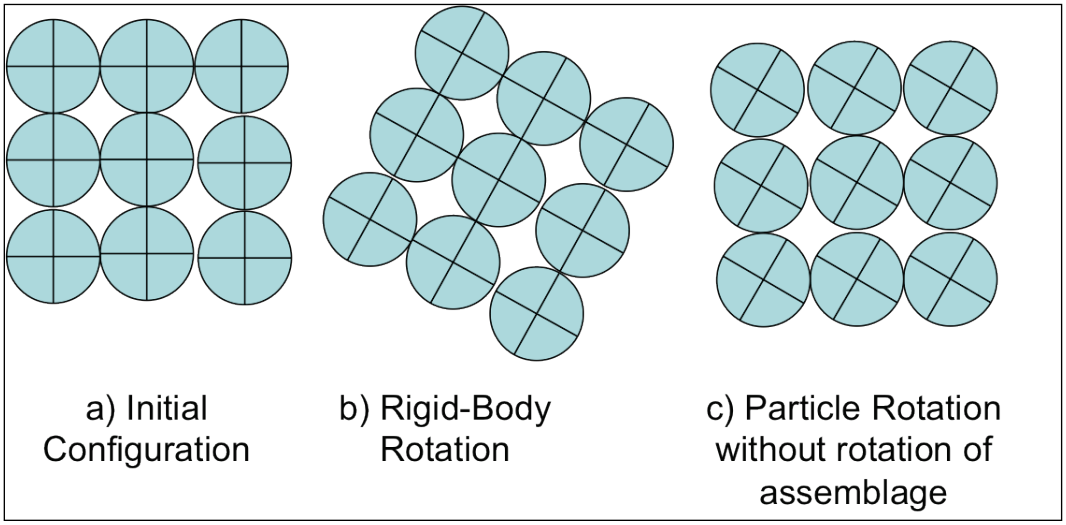

Particle rotation is especially important for development of instability such as with the formation of shear bands. Forces are transmitted through particle chains that can fail as a result of slipping at contacts or through buckling of the force chains. These motions are thus an interplay between particle translation and rotations, as illustrated in Figure 5. Figure 6 illustrates two extreme combinations of particle translation and rotation that can develop during simple shear. Note that the degree of contact motion is the same for these two cases. Uniform free rotation induces even greater contact motion. Therefore, the effective strain in a granular media can be viewed as having components related to both the strain, as defined by the velocity field followed by particle centers, and the rotation of the particles about their centers,

Figure 5. Particle rotations cause by buckling deformation such as occurs in shear band formation: (a) without particle rotation; (b) with particle rotation.

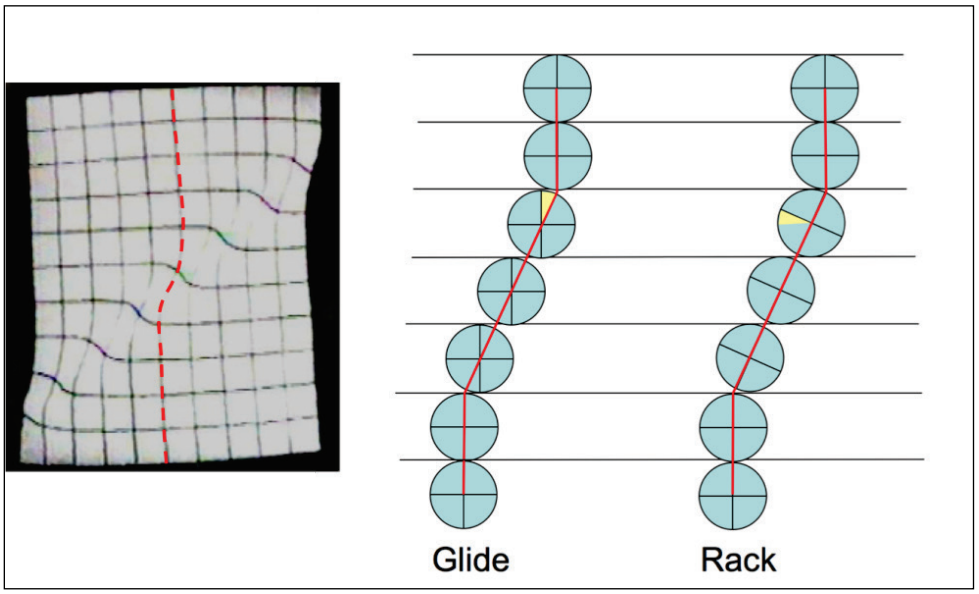

Figure 6. Effects of various combinations of particle rotations and deformation on the contact displacements: (a) pure deformation without particle rotation; (b) deformation with particle rotation; and (c) no deformation and particle rotation. The dislocation of the contacts depends on a combination of shear deformation and particle rotation.

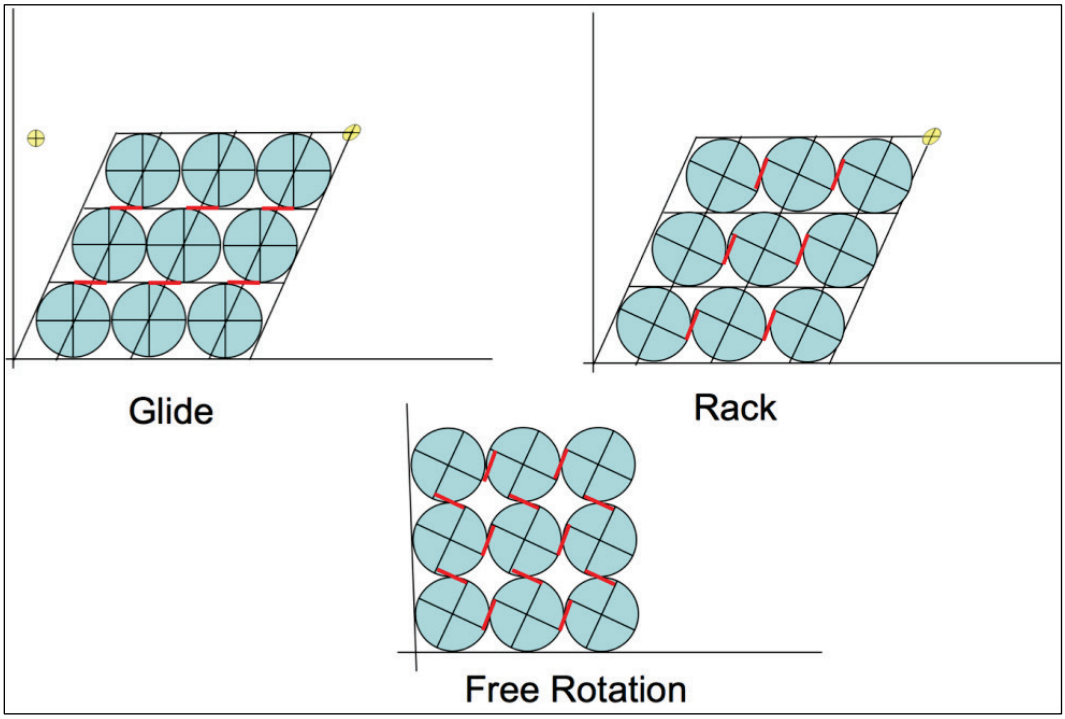

$$\varepsilon_{ij} = \varepsilon_{ij} - \varepsilon_{ijk}\omega_k \tag{11}$$

where ε_{ij} is the strain field defined by

$$\varepsilon_{ij} = \frac{1}{2}\left(\frac{\partial_{v_i}}{\partial_{x_j}} + \frac{\partial_{v_i}}{\partial_{x_i}}\right) \tag{12}$$

which is symmetric with respect to interchanging i and j, and the rotational part $e_{ijk}\omega_k$, which is anti-symmetric given that $e_{ijk}\omega_k = -e_{jik}\omega_k$. The rotation ω_k is an independent degree of freedom, separate from the rigid-body rotation of the neighborhood given by the anti-symmetric part of the velocity gradient

$$\omega_{ij} = \frac{1}{2}\left(\frac{\partial_{v_i}}{\partial_{x_j}} - \frac{\partial_{v_j}}{\partial_{x_i}}\right). \tag{13}$$

When describing a granular media, ω_k presumably represents the particle rotation after subtracting the rigid-body rotation of the assemblage.

In addition to the particle rotation, the rotation gradients, or flexure modes shown in Figure 7, contribute to the constitutive response of the material. As with other deformation modes discussed, flexure can involve combinations of particle displacement and rotation of the particle. For each flexure degree of freedom, there is a conjugate couple, as shown in Figure 8 for one face of an element.

Figure 7. Gradients in rotation caused by flexure: (a) rotation caused by motion of particle centers; (b) flexure motion without particle rotations; and (c) rotation gradient without flexure motion.

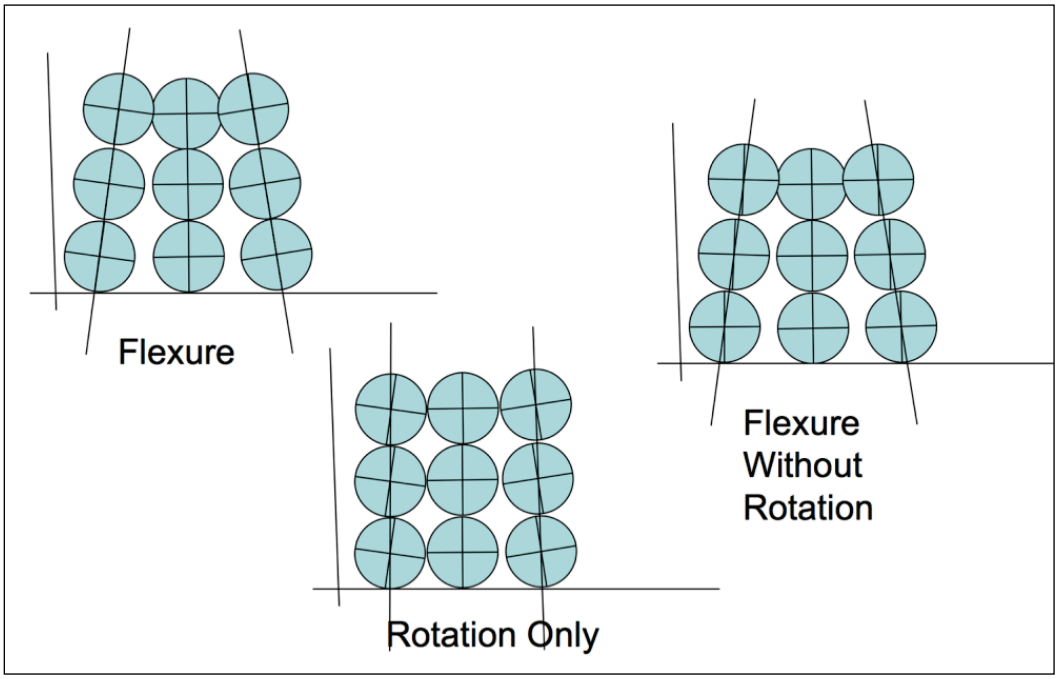

Figure 8. The stress, σ_{11} and σ_{12}, and couple, $\mu_{13,}$ acting on the x_1 face of an element. The element is shown deformed from its original configuration as a result of strain, ε_{11} and ε_{12}, and rotation gradient, κ_{31}.

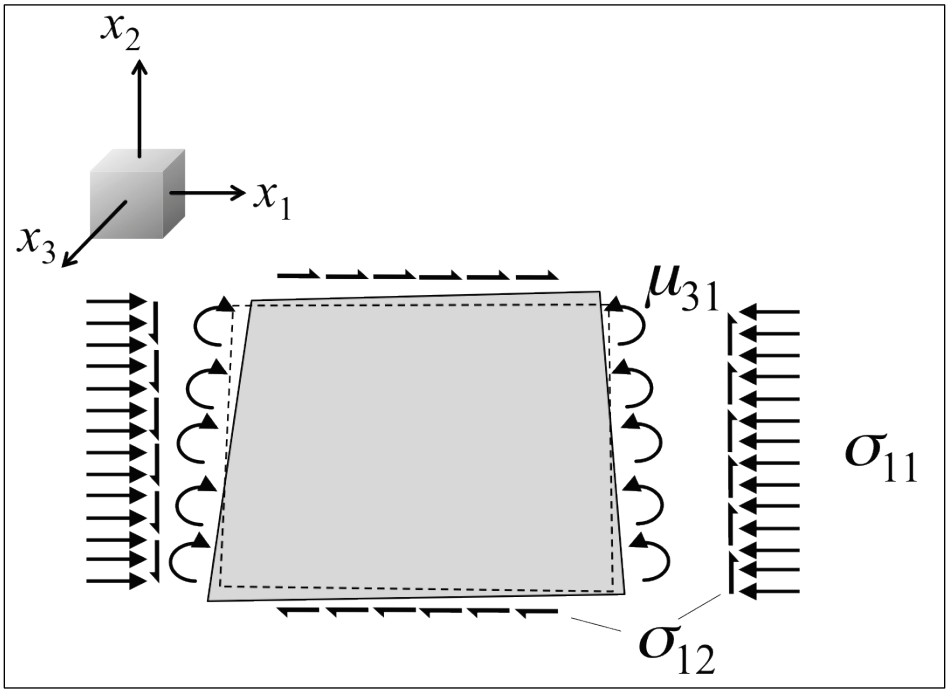

2.8 Virtual power and strain rates

All energy is either stored or dissipated by relative motion at contacts. Given the virtual motion of two particles and the contact force, the power at the contact is $\delta v_i^c f_i^c$, where the virtual motion at the contact is

$$\delta v_i^c = \delta v_i^{A_c} - \delta v_i^{B_c} + e_{ijk}\left(r_i^A \delta\omega_j^{A_c} - r_i^B \delta\omega_j^{B_c}\right). \tag{14}$$

The relative motion at the contact depends on the differences in linear displacements and rotations between contacting particles. In a continuum, the rotation is computed from the velocity field. Here, the rotations of the particles are independent and not tied to the rotation of the neighborhood. Therefore, an independent kinematic quantity describing the particle rotations must be included in the continuum formulation. This quantity is a thermodynamic conjugate to the couple $\bar{\mu}_{ij}$, necessitating an additional momentum balance relationship associated with the Cosserat continuum theory. That is, a Cosserat-like relationship should be anticipated based on the particle kinematics alone. For the purpose of this introduction, the Cosserat couples are assumed to be negligible. The complete system of stresses and couples will be addressed in Chapter 4.

The continuum kinematics can be inferred from the discrete relationships by requiring equality between the virtual power of the continuum and that of the discrete material. The power balance is given by

$$V\bar{\sigma}_{ij}\delta\dot{\varepsilon}_{ij} = \sum_{c=1}^{N_c}\left(\delta u_i^A - \delta u_i^B + e_{ijk}\left(r_i^A \delta\omega_j^A - r_i^B \delta\omega_j^B\right)\right) f_i^c \tag{15}$$

From the assumption that the Cosserat couples are negligible, we assume that the sum of the moments is likewise zero,

$$\sum_{c=1}^{N_c} e_{ijk}\left(r_i^A \delta\omega_j^A - r_i^B \delta\omega_j^B\right) f_i^c = 0. \tag{16}$$

Substituting Equation (8) into the power balance relationships and making use of the identity (1), we get

$$V\left(\sum_{c=1}^{N_c}\left(r_j^{A_C}-r_j^{B_c}\right)f_i^c\right)\delta\dot{\varepsilon}_{ij}=\sum_{c=1}^{N_c}\cdot\left(\delta u_i^A-\delta u_i^B\right)f_i^c \tag{17}$$

Noting that f_i^c appears on both sides of each equation, we can write

$$\sum_{c=1}^{N_c}\left[V\left(r_j^{A_C}-r_j^{B_c}\right)\delta\dot{\varepsilon}_{ij}-\left(\delta u_i^A-\delta u_i^B\right)\right]f_i^c=0 \tag{18}$$

In principle, the definition of strain should be independent of the contact forces. Therefore, Equation (18) must be satisfied for all f_i^c implying that the quantity in brackets must be zero for *all* contacts. This condition would be met if the particle centroids follow the affine deformation defined by the constant strain increment $\delta\varepsilon_{ij}$. In general, particle motions are not affine, implying the product $\sigma_{ij}\delta\varepsilon_{ij}$ does not account for all of the work done by forces at the contacts. We must therefore recognize that no definition of $\delta\varepsilon_{ij}$ will satisfy the power balance exactly in view of the arbitrary nature of the contact forces. Thus, the problem must be addressed by finding a general procedure to yield proper work conjugates that includes both translational and rotational motions.

3 Extraction of Kinematic Variables

3.1 Rigid-body motions and deformation

For an assemblage of particles, the following statements are equivalent:

- Relative contact motions are zero.
- The motion of particle centers is the sum of a translation and a rotation common to all particles within the assembly.

The first statement relates to the constitutive behavior of the body. The change in energy state of the assemblage is changed by relative motion of contact pairs. The relative motion between two particles designated A and B is given by Equation (14) from which it follows that no contact motion occurs when

$$v_i^A - v_i^B = -e_{ijk}\left(r_j^A \omega_k^A - r_j^B \omega_k^B\right) \tag{19}$$

Such motions correspond to rigid-body motion of the particle pair. The second statement follows immediately from the first. Both statements are related to the observation that physical laws governing a body are invariant to rigid-body motions, these motions being equivalent to motions of the observer relative to the body. The invariance of physical law to observer motion is referred to as the symmetry of physical law; in mechanics, the principle is referred to as objectivity. The principle forms the basis of describing deformation of discrete particle systems. Any operator defined to extract deformation measures from particle motions is orthogonal to rigid-body motions (Peters 2005). Thus, a vector space can be defined from which all admissible deformations can be constructed as a linear combination of vectors that are orthogonal to the rigid body motions given by

$$u_i(\mathbf{x}) = u_i(0) + e_{ijk} x_j \omega_k(0). \tag{20}$$

For each set of admissible deformation vectors, there is a conjugate set of "stress" vectors. The practical value of any of these quantities depends on the application at hand. For engineering applications, the interest is generally in defining an equivalent continuum, in which case it is natural to decompose the deformation space into projected continuum motion and *independent* motions. Adopting matrix notation described in detail

in Section 3.2, the projected and independent motions can be expressed by Peters and Walizer (2013)

$$\mathbf{v} = \mathbf{Le} + \mathbf{v}_{\mathrm{i}}, \tag{21}$$

where velocities and rotation rates of particles in the assemblage are arranged in $\mathbf{v}$, $\mathbf{L}$ is the projection matrix for the continuum motions $\mathbf{e}$, and $\mathbf{v}_i$ is the matrix of independent motions.* The continuum motions $\mathbf{e}$ contain rigid-body motions as well as deformations, shown in Figure 9. The term *independent* is used without reference to the phenomena causing the motion (e.g., diffusion) and is characterized by the relation

Figure 9. Velocity field produced by projecting a uniform strain ($v_i = \dot{\varepsilon}_{ij}x_j$ or equivalently $\mathbf{v} = \mathbf{Le}$) (from Peters and Walizer 2013).

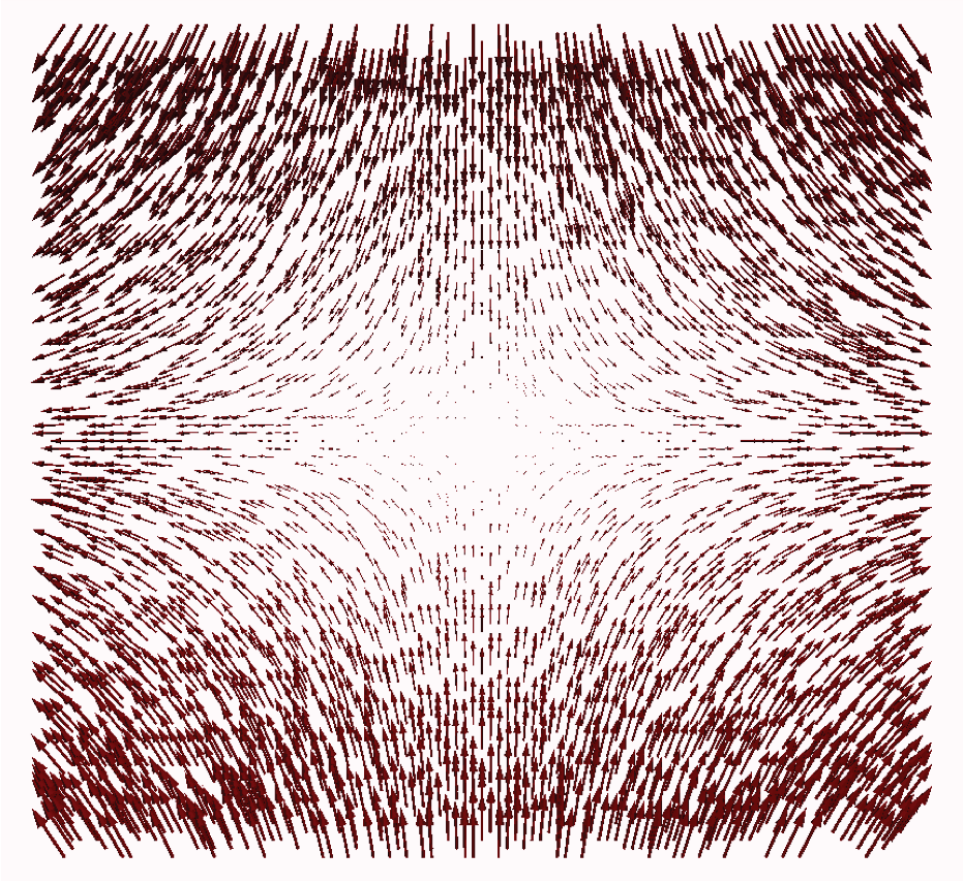

$$(\mathbf{v}_i)^T\mathbf{Le} = 0. \tag{22}$$

* The subscript *i* on v_i donates "independent" and is not a Cartesian component.

Equation (22) is satisfied by minimizing the magnitude of the independent motions given as the quantity R^2,

$$R^2 = (\mathbf{v}_i)^T \mathbf{v}_i. \tag{23}$$

The minimization amounts to defining **e** as the least-square approximation to the total motion, given by the condition

$$\mathbf{L}^T(\mathbf{v} - \mathbf{L}\mathbf{e}) = 0 \tag{24}$$

The affine motions of the continuum are thus given by

$$e = (\mathbf{L}^T\mathbf{L})^{-1}\mathbf{L}^T\mathbf{v}. \tag{25}$$

It can be verified by substitution of Equation (21) and (24) that $\boldsymbol{L}^T\mathbf{v}_i = \mathbf{0}$, which is a sufficient condition to satisfy Equation (22). The definition of the projection operator **L** includes the rigid-body modes. Thus, the orthogonality condition, Equation (22), insures $\mathbf{v}_i$ satisfies the principle of objectivity.

The structure of the projection is such that the columns of **L** form a subspace of base vectors, linear combinations of which make up all possible projected motions. The deformation measures **e** are the weighting to those vectors. Similarly, the independent motions, $\mathbf{v}_i$, can be expressed as a linear combination of N^i base vectors that make up the subspace in independent motions,

$$\mathbf{v}_i = \sum_{r \epsilon N^i} e_r^i \mathbf{p}_i. \tag{26}$$

where e_r^i are multipliers to the mutually orthogonal base vector $\mathbf{p}_i$. The columns of **L** and the vectors $\mathbf{p}_i$ together span the space of all possible motions of particles in the assemblage; **L** defines the possible affine motions whereas $\mathbf{p}_i$ constitutes non-affine motions with $\boldsymbol{L}^T\mathbf{p}_i$ for all i. For each multiplayer e_r^i, there is a conjugate force s_i such that the product $s_i e_i$ (no repeated sum on i) is the work done by the i^{th} non-affine mode. The non-affine modes are not investigated in this study, but it should be noted that much of the inelastic behavior observed in the discrete material is a result of non-affine motions (Walsh et al. 2007).

3.2 Data structures

The structure of **L** is based on the ordering of terms in **e**, which is as follows:

$$\mathbf{e}^{\mathrm{T}} = \begin{Bmatrix} v_x^o, v_y^o, v_z^o, \omega_x^o, \omega_y^o, \omega_z^o, \varepsilon_{xx}, \varepsilon_{yy,}\varepsilon_{zz}, \varepsilon_{xy}, \varepsilon_{yz}, \varepsilon_{xz}, \omega_x, \omega_y, \omega_z, k_{xx}, \\ k_{yy}, k_{zz}, k_{xy}, k_{xz}, k_{yx}, k_{yz}, k_{zx}, k_{zy} \end{Bmatrix}, \quad (27)$$

and the ordering of $\mathbf{v}_p$, which is as follows:

$$\mathbf{v}_p^T = \{v_x, v_y, v_z, \omega_x, \omega_y, \omega_z\}. \quad (28)$$

The variables v_x^o, v_y^o, and v_z^o are the three components of rigid-body translational motion; ω_x^o, ω_y^o, and ω_z^o are the three components of rigid-body rotation; ε_{ij} are the six components of strain representing the symmetric part of the strain tensor; ω_i are the three components of particle rotation that define the anti-symmetric part of the strain tensor; and κ_{ij} are the nine components of the rotation gradient tensor. The subscript p refers to the particle in question. The vector **v** is a collection of all $\mathbf{v}_p$. The vector **e** can be expressed in terms of sub-groups given by

$$\mathbf{e}^T = \{\mathbf{v}^o, \mathbf{w}^o, \mathbf{e}^s, \mathbf{w}^a, \mathbf{k}\}. \quad (29)$$

Similarly, $\mathbf{v}_p$ can be grouped as

$$\{\mathbf{v}_p, \mathbf{w_p}\}^T = \left\{\{v_1^p, v_2^p, v_3^p\}, \{w_1^p, w_2^p, w_3^p\}\right\}. \quad (30)$$

The matrix **L** contains a sub matrix $\mathbf{L}_p$ for each particle. The structure of $\mathbf{L}_p$ can be visualized by the following tabulation, which shows the projected motions in the left-most column, the continuum motions in the top row, and the elements of $\mathbf{L}_p$ in the table:

	$\mathbf{v}^o$	$\mathbf{w}^o$	$\mathbf{e}^s$	$\mathbf{w}^a$	$\mathbf{k}$
$\mathbf{v}_p$	**I**	$\mathbf{R}^p$	$\mathbf{x}^p$	**o**	**o**
$\mathbf{w}_p$	**o**	**I**	**o**	**I**	$\mathbf{x}^{\mathrm{pk}}$

where **I** is a 3×3 identity matrix, **o** a matrix of zeros, and

$$\mathbf{R}^p = \begin{bmatrix} 0 & z & y \\ z & 0 & -x \\ -y & -x & 0 \end{bmatrix}^p$$

$$\mathbf{x} = \begin{bmatrix} x & 0 & 0 \\ 0 & y & 0 \\ 0 & 0 & z \end{bmatrix}^p$$

$$\mathbf{x}^{pk} = \begin{bmatrix} x & 0 & 0 & y & 0 & z & 0 & 0 & 0 \\ 0 & y & 0 & 0 & x & 0 & 0 & z & 0 \\ 0 & 0 & z & 0 & 0 & 0 & x & 0 & y \end{bmatrix}^p .$$

The coordinates (x,y,z) mark the center of the particle p relative to the center of the REV.

3.3 Stress

Just as the particle velocities can be expanded into modes, the particle forces can be expressed as

$$\mathbf{f} = \mathbf{L}\mathbf{s} + \sum_{r \epsilon N^i} s_r^i \mathbf{p}_i, \tag{31}$$

noting that $\mathbf{L}$ and $\mathbf{p}^i$ spans the space of all $\mathbf{f}$. In view of the orthogonality between $\mathbf{L}$ and $\mathbf{p}^i$, the power within the REV is given by

$$\mathbf{f}^T \delta\mathbf{v} = V\left(\mathbf{s}^T\mathbf{L}^T\mathbf{L}\delta\mathbf{e} + \sum_{r \epsilon N^i} s_r^i \delta e_r^i\right). \tag{32}$$

The work conjugate to $\delta\mathbf{e}$ is $\mathbf{s}^T\mathbf{L}^T\mathbf{L}$. Noting that $\mathbf{s} = (\mathbf{L}^T\mathbf{L})^{-1}\mathbf{L}^T\mathbf{f}$, the "stress" that is conjugate to $\delta\mathbf{e}$ is seen to be equal to

$$\mathbf{t} = \frac{1}{V}(\mathbf{L}^T\mathbf{f}). \tag{33}$$

The stress $\mathbf{t}$ includes the conjugates to ε_{ij}, ω_i, and κ_{ij}. The detailed derivation of these quantities is presented in the Chapter 4.

The force and moments quantities in Equation (33) are illustrated in Figure 10. The forces and moments acting at particle centers are zero everywhere except for boundary particles. The forces and moments acting on the boundary particles are statically equivalent to the forces acting at

the bounding contacts. In effect, summation of these quantities amounts to a surface integration because the particles having non-zero quantities are nominally at the surface of the REV.

Figure 10. Relationship between forces acting on the boundary of a sample volume and at the particle centers when only contacts internal to the volume are considered. Under static conditions, contact forces are all at equilibrium making the forces at particle centers to be zero. When the forces on the volume boundaries are excluded, statically equivalent forces must be applied to the centers of particles at the volume boundaries.

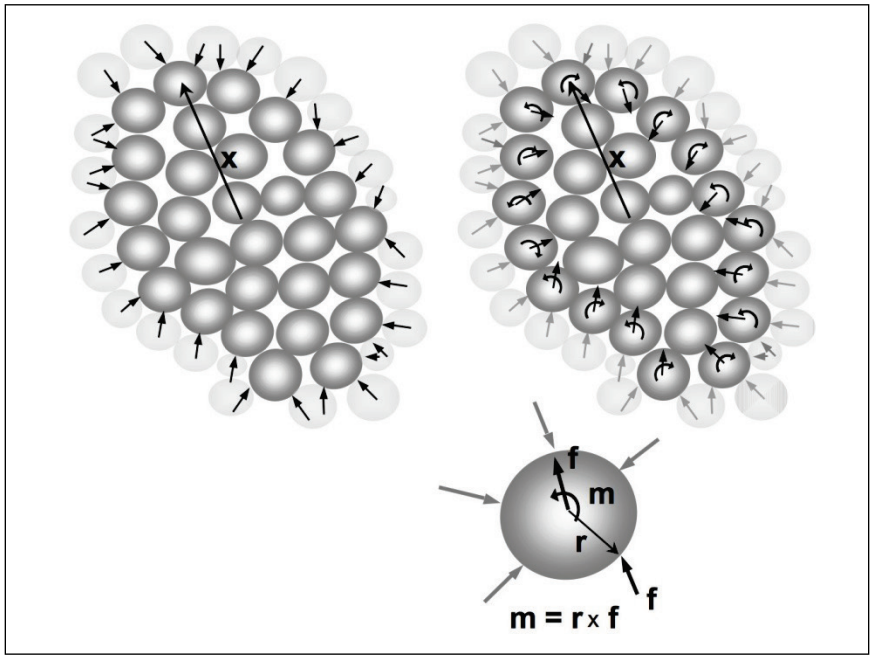

4 Work-Consistent Average Stress and Couple

It was shown in the previous chapter that a work-consistent definition of stress can be obtained from the least-square formalization. What is sought are definitions of stress and couple consistent with the Cosserat continuum. To that end, a direct application of the virtual work method is used to derive specific relationships for the stress and couple tensors. At the end of the section, the correspondence between the least-square definition of stress and the quantities derived from the direct approach are presented.

The virtual work balance for the REV in terms of continuum variables and discrete variables can be written as

$$\begin{aligned}\delta W &= \sum_{p\epsilon N^p}\left[\delta u_i^p \sum_{c\epsilon M^p} f_i^c + \delta\omega_i^p\left(e_{ijk}\sum_{c\epsilon M^p} r_j^c f_k^c + m_i^p\right)\right] \\ &= V\left(\sigma_{ij}\delta\varepsilon_{ij} + \mu_{ij}\delta\kappa_{ij}\right).\end{aligned} \tag{33}$$

The expression for the work by the discrete variables can be simplified through use of the properties between particle-based sums and contact-based sums. First note that the radius vector r_i^c is the difference between the coordinate of the particle center and the coordinate of the contact,

$$r_j^c = x_j^p - x_j^c \tag{35}$$

Thus,

$$\delta W = \sum_{p\epsilon N^p}\left[\delta u_i^p \sum_{c\epsilon M^p} f_i^c + \delta\omega_i^p\left(e_{ijk}\sum_{c\epsilon M^p}\left(x_j^p - x_j^c\right)f_k^c + m_i^p\right)\right]. \tag{36}$$

With reference to Figure 10, the contacts in the sampling region represent particle pairs whereas those on the boundary can be viewed as applied forces and moments. For the $\overline{N}^p$ interior contacts the terms associated with the contact vector x_i^c can be removed using the identity

$$\sum_{p\epsilon N^p}\sum_{c\epsilon M^p} x_j^c f_k^c = \sum_{c\epsilon N^c}\left(x_j^{A_c} - x_j^{B_c}\right) f_k^c = 0, \tag{37}$$

because $x_j^{A_c} = x_j^{B_c}$. Also

$$f_i^p = \sum_{c\epsilon M^p} f_i^c. \tag{38}$$

and Figure 11.

Figure 11. The relationships among r_j^c, x_j^p, and x_j^c for the A and B particles. The vector x_j^c points to the contact and is therefore common to both particles.

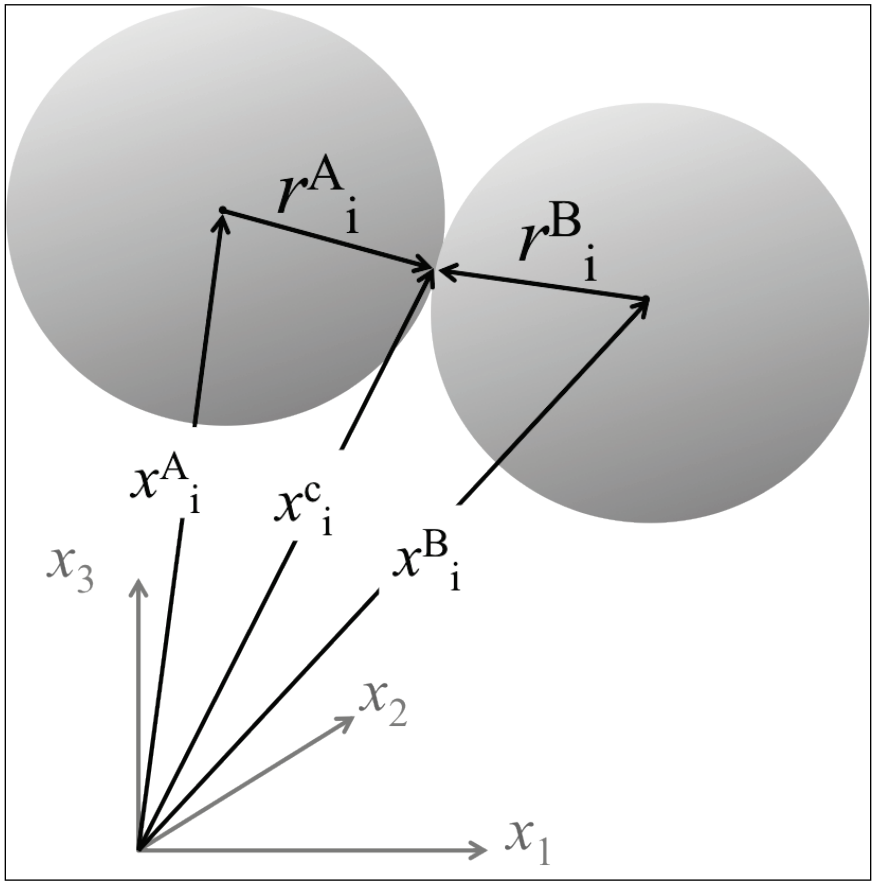

Thus, the expression can be simplified to

$$\delta W = \sum_{p\epsilon N^p}\left[\delta u_i^p f_i^p + \delta\omega_i^p\left(e_{ijk} r_j^c f_k^p + m_i^p\right)\right]. \tag{39}$$

The projection of the discrete variables from the continuum variables are given as

$$\begin{aligned} \delta u_i^p &= \delta \varepsilon_{ij} x_j^p \\ \delta \omega_i^p &= \delta \omega_i + \delta \kappa_{il} x_l^p \end{aligned} \tag{40}$$

Substituting the projected variables into the work expression gives

$$\begin{aligned} \delta W = \delta \varepsilon_{ij} \sum_{p \epsilon N^p} x_j^p f_i^p + \delta \omega_i \sum_{p \epsilon N^p} \left(e_{ijk} r_j^c f_k^p + m_i^p \right) \\ + \delta \kappa_{il} \sum_{p \epsilon N^p} x_l^p \left(e_{ijk} r_j^c f_k^p + m_i^p \right). \end{aligned} \tag{41}$$

The work relationship can now be expressed in terms of the total strain variable given by Equation (11). Also, noting it is a contact-based sum and that the contact moments balance each other, that is, can eliminate the moment associated with the Cosserat rotation,

$$\begin{aligned} \sum_{p \epsilon \bar{N}^p} m_i^p &= \sum_{p \epsilon N^p} \sum_{c \epsilon M^p} m_i^c \\ &= \sum_{p \epsilon N^c} \left(m_i^{A_c} + m_i^{B_c} \right) \\ &= \sum_{p \epsilon N^c} \left(m_i^{A_c} - m_i^{A_c} \right) \\ &= 0. \end{aligned} \tag{42}$$

Inserting Equation (11) into Equation (41) and in view of Equation (42), the work of the discrete motions and forces becomes

$$\delta W = \delta \varepsilon_{ij} \sum_{p \epsilon N^p} x_j^p f_i^p + \delta \kappa_{il} \sum_{p \epsilon N^p} \left(e_{ijk} x_l^p r_j^c f_k^p + x_l^p m_i^p \right). \tag{43}$$

In deriving Equation (43) it is necessary to deal with the term

$$\delta\omega_i \sum_{p\epsilon\widehat{N}^p} \left(e_{ijk} x_j^c f_k^p + m_i^p\right)$$

where $\widehat{N}^p$ refers to the particles on the boundary of the sampling area. Whereas δw_i refers to a total rotation, the summation taken over all particles on the boundary is zero.

Returning to Equation (34), we equate terms respectively multiplied by ε_{ij} and κ_{ij} to obtain the conjugate stress variables

$$\sigma_{ij} = \frac{1}{V} \sum_{p\epsilon N^p} x_j^p f_i^p \tag{44}$$

and

$$\mu_{il} = \frac{1}{V} \sum_{p\epsilon N^p} \left(e_{ijk} x_l^p r_j^c f_k^p + x_l^p m_i^p\right). \tag{45}$$

Equation (44) is clearly in the form of the particle stress given in Equation (8), but with the sum taken over the surface of the sampling area. Equation (45) is a similar sum except the particle forces are replaced with the total moment acting on each boundary particle.

5 Example Data Extraction

A subroutine was prepared in Fortran 95 to extract the kinematic and stress quantities. The procedure to obtain the kinematic variables is a direct implementation of Equation (25). The conjugate stresses were obtained from Equation (33).

5.1 Sampling algorithm

The subroutine allows two methods to define an REV. In both methods, a point is defined as a nominal center of the sample volume along with its size. Either a cubical or spherical sampling volume can be specified. In the case of the cubical sampling volume, the sampling size represents the side length; in the case of the spherical volume, the size represents the radius. In both cases, a loop is made through the contact list to determine if the contact falls within the sample volume. It is then determined if both A and B particles fall within the sample volume. If both particles lie within the sample volume, the contact is marked as internal and added to the list. If only one of the particles lies within the volume, the contact is external and ignored. The **v** and **L** arrays are constructed using the particle center coordinates, displacement, and rotation to implement Equation (25). The contact forces and moments are added to the particle quantities using the usual assembly process, which builds the **f** vector for application of Equation (33). The individual quantities ε_{ij}, ω_i, and κ_{ij} are extracted from **e** as well as the rigid-body displacement and rotation. The quantities σ_{ij} and κ_{ij} are extracted from **t**. The forces and moments associated with the rigid-body moments are also extracted as a check, whereby both should be zero for static conditions.

5.2 Test case

The subroutine was tested by simulating a three-dimensional rigid-wall, a 6-in. × 6-in. × 6-in. cube, as shown Figure 12. The initial particle placement was obtained using the particle generation algorithm, which is a companion preprocessor to DEM. During the particle generation phase, an initial internal stress state was imposed on the particles as they grew into contact with each other and the cube's rigid wall faces. A uniaxial displacement of 0.4 in. was then applied using the top wall face for three separate test cases. The REV samples of various particle sizes were taken from the cube's center. The particles inside the REV spherical sample volume were used to compute the strains and stresses for each test case. Provided in Table 1 are the properties for the cube, particles, and REV.

Figure 12. Illustration of three-dimensional 6 in. × 6 in. × 6 in rigid wall cube.

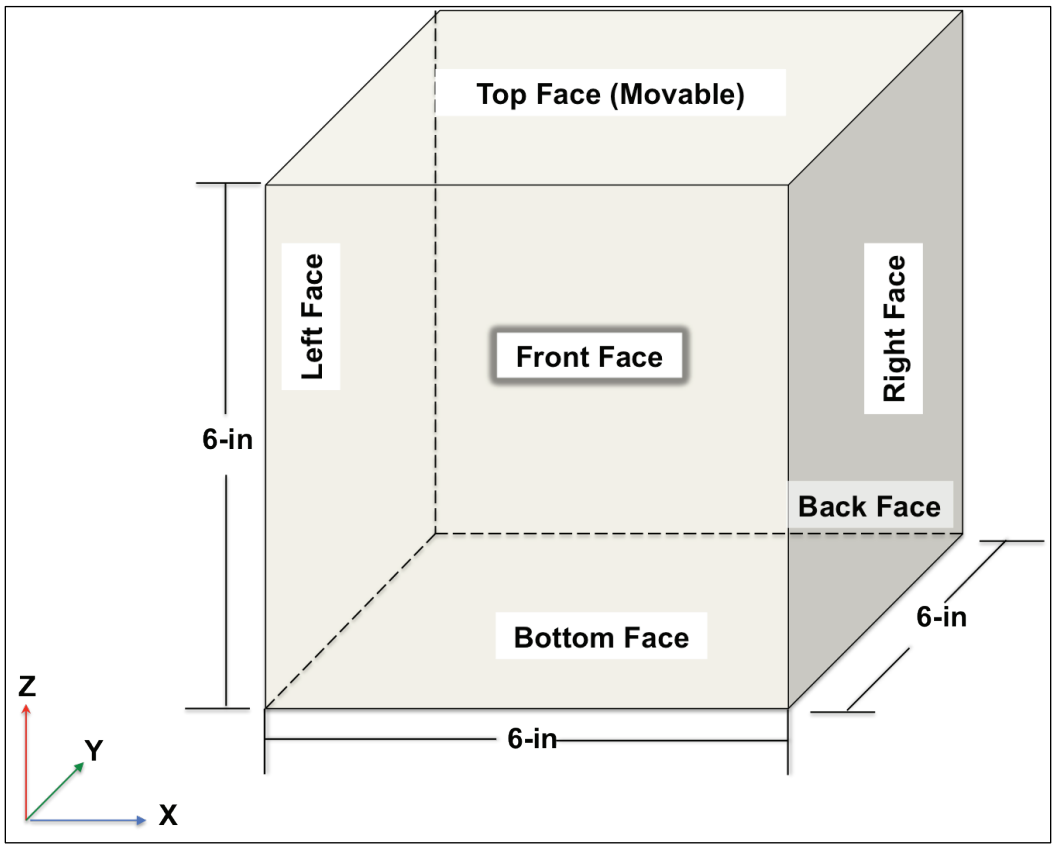

As a reference, the wall and REV 'stress' were computed from the applied forces on the movable upper-wall face and the strains were computed from the movable upper-wall face displacements. Provided in Tables 2 through 4 for Figures 13 through 15 are the computed properties for stress and strain for test cases 1 through 3. Cases 1, 2, and 3 contain approximately 9,000, 18,000, and 27,000 spherical particles, respectively.

In general, the extracted strains agreed well with those computed from the boundary motions. The relative stresses agreed well with those computed from the boundary forces, although the magnitudes of the extracted stresses were lower than those derived from the rigid walls boundary. There was disparity between the wall and REV stress determinations for the spherical sample volumes. The repeatability of the stress results for all sample shapes and sizes suggests an inherent difference between internal stresses and boundary stresses for this test. It is known that the use of rigid platens imposes a boundary condition in which the particles align to each platen surface, creating a dense array of force chains through which higher-than-average forces are transferred between opposing platens.

Table 1. Properties for cube, particles, and REV.

Properties	Cube Case #1	Cube Case #2	Cube Case #3
Cube Volume (in.^{3})	192.00	192.00	192.00
Total Spherical Particle Count in Cube	9,029	18,015	27,025
Particle Contacts	16,099	32,195	49,096
Minimum Particle Size Radius (in.)	0.14	0.08	0.06
Maximum Particle Size Radius (in.)	0.31	0.23	0.22
Average Particle Size Radius (in.)	0.24	0.19	0.16
REV Sample Radius Size (in.)	2.00	2.00	2.00
REV (in.^{3})	33.51	33.51	33.51
Total Spherical Particle Count in REV	275	575	853
REV Solids (in.^{3})	19.19	19.69	19.33
REV Porosity (%)	42.72	41.24	42.32
REV Particle Contacts	407	907	1,347

Figure 13. Case 1 showing cube with approximately 9,000 spherical particles.

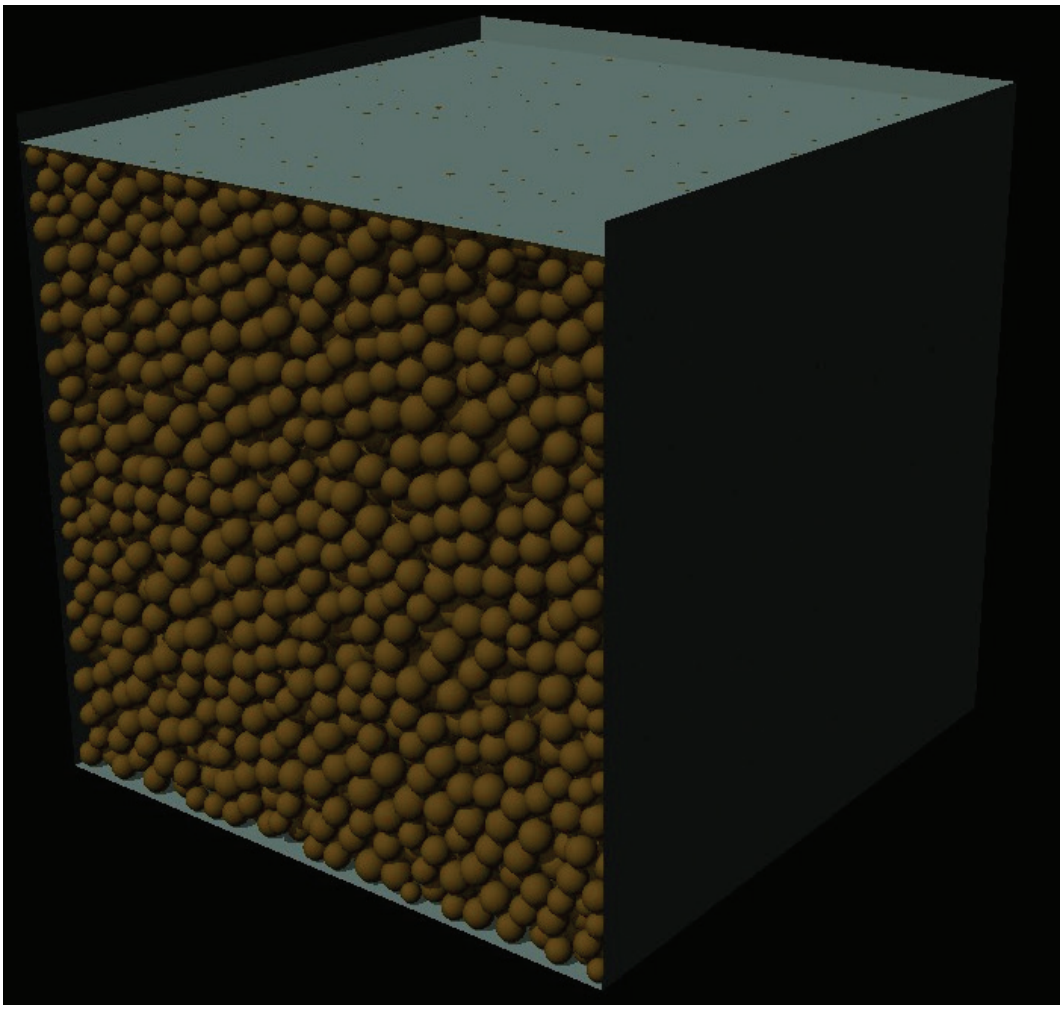

Table 2. Computed strains and stresses for wall and REV for 9,000 spherical particles case.

Wall Stresses			
Average Stress Tensor (psi)			
Wall Face	x	y	z
Bottom	9.82	-3.01	-696.97
Top	-16.49	10.96	969.67
Back	2.14	-167.04	-85.27
Front	3.85	148.22	-75.84
Left	-161.24	-0.52	-82.44
Right	162.82	3.11	-82.96
REV Strains and Stresses			
	Linear Strain Tensor (in./in.) × 10^{-2}		
	x	y	Z
x	-1.71	-0.75	0.02
y	-0.75	0.52	0.36
z	0.15	0.36	-36.52
	Cosserat Coupled Stress Tensor (psi)		
	x	y	Z
x	5.54	-9.01	-0.02
y	61.77	-99.65	-0.21
z	0.08	-0.13	0.00
	Linear Stress Tensor (psi) × 10^{-2}		
	x	y	Z
x	0.00	0.00	5.32
y	0.00	0.00	-8.65
z	5.32	-8.65	-0.01

Figure 14. Case 2 showing cube with approximately 18,000 spherical particles.

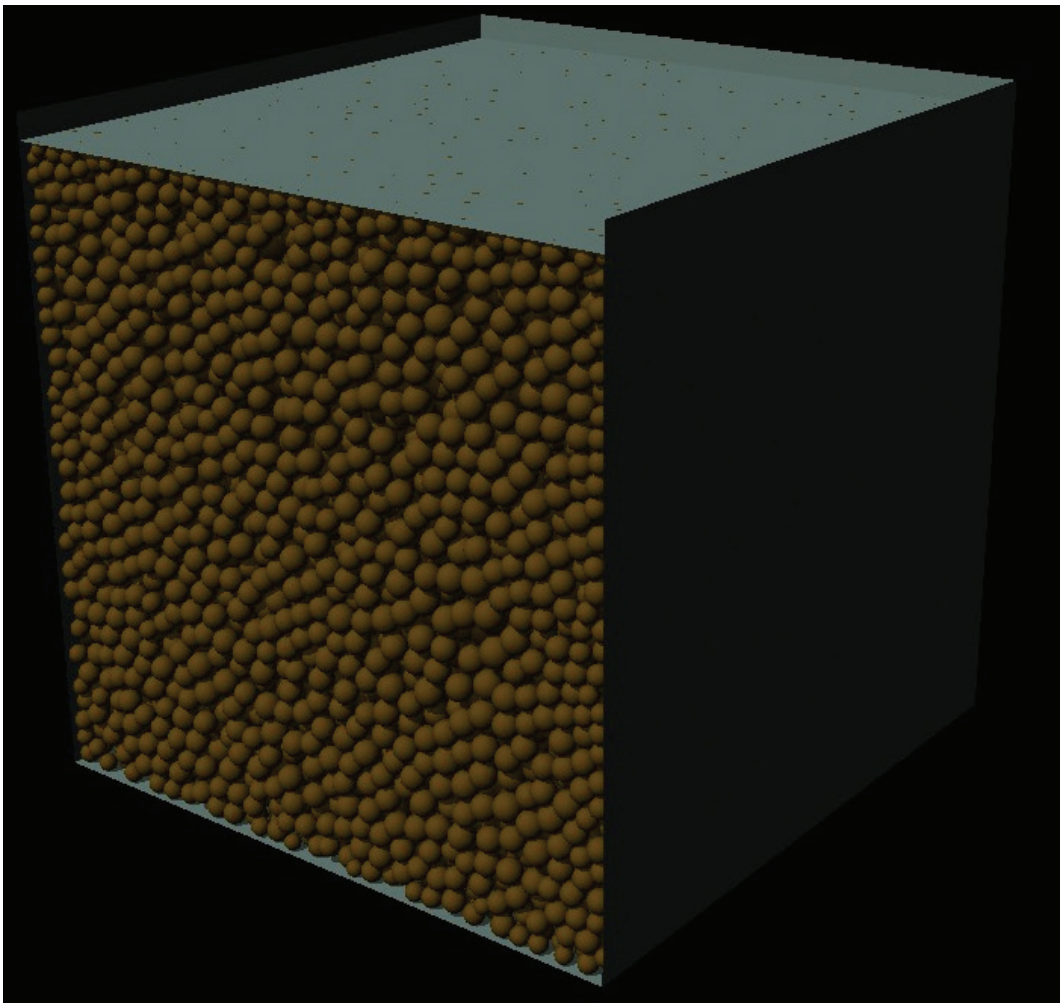

Table 3. Computed strains and stresses for wall and REV 18,000 spherical particles case.

Wall Stresses			
	Average Stress Tensor (psi)		
Wall Face	x	y	z
Bottom	-8.06	-1.83	-889.31
Top	-8.43	26.31	1253.53
Back	1.35	-214.91	-110.22
Front	0.19	191.66	-98.66
Left	-192.88	0.31	-99.70
Right	207.88	-1.16	-106.83
REV Strains and Stresses			
	Linear Strain Tensor (in./in.) × 10^{-2}		
	x	Y	Z
x	-0.53	1.49	2.57
y	1.49	2.00	2.31
z	2.57	2.31	-37.57
	Cosserat Coupled Stress Tensor (psi)		
	x	Y	Z
x	0.75	-0.38	0.41
y	117.61	-59.52	63.84
z	-2.35	1.19	-1.28
	Linear Stress Tensor (psi) × 10^{-2}		
	x	y	z
x	0.00	0.00	8.20
y	0.00	0.00	-4.15
z	8.21	-4.15	4.45

Figure 15. Case 3 showing cube with approximately 27,000 spherical particles.

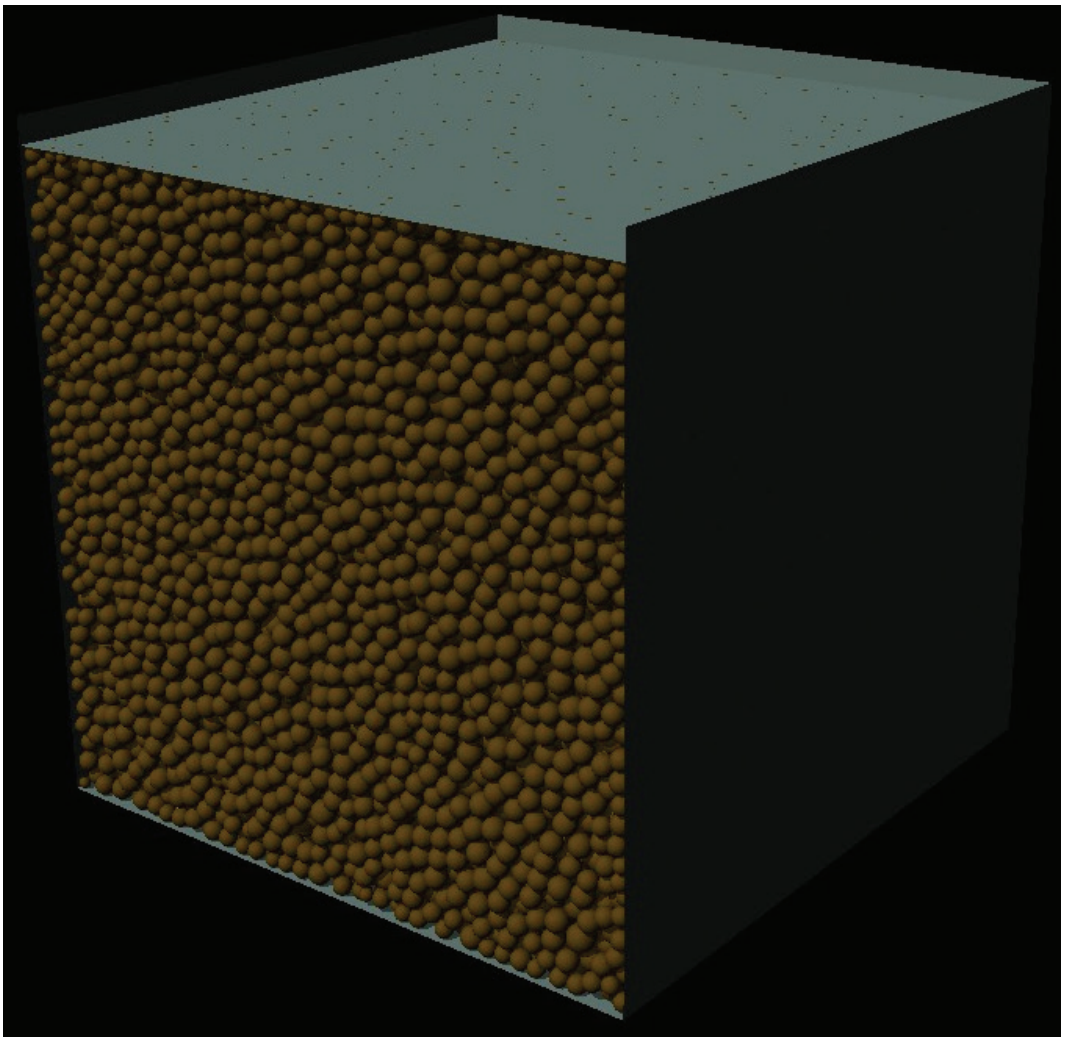

Table 4. Computed strains and stresses for wall and REV for 27,000 spherical particles case.

Wall Stresses			
	Average Stress Tensor (psi)		
Wall Face	x	y	z
Bottom	2.08	10.45	-1234.77
Top	-8.63	4.73	1739.34
Back	2.04	-279.51	-142.89
Front	1.08	267.50	-136.99
Left	-271.50	-1.92	-139.32
Right	274.73	-1.08	-140.38
REV Strains and Stresses			
	Linear Strain Tensor (in./in.) × 10^{-2}		
	x	y	Z
x	1.00	0.17	-1.15
y	0.17	0.27	-0.69
z	1.15	-0.69	-42.30
	Cosserat Coupled Stress Tensor (psi)		
	x	y	Z
x	-1.69	3.60	-1.41
y	75.61	-161.23	63.51
z	0.66	-1.41	0.56
	Linear Stress Tensor (psi) × 10^{-2}		
	x	y	Z
x	0.00	0.00	4.52
y	0.00	0.00	-9.64
z	4.52	-9.64	3.88

6 Conclusions/Recommendations

The discrete element method (DEM) provides a realistic approach to modeling materials at fundamental length scales. Materials at the *discrete scale* can be the particle size in granular materials such as sand, micrometer sizes when dealing with polycrystalline materials, or nanometer sizes when dealing with biologic materials. At such scales, complex material behavior can be simulated as relative simple interactions between discrete entities, obviating the need for sophisticated phenomenological constitutive models. The ultimate goal is to obtain the engineering behavior at the prototype scale at which problems are formulated in terms of continuum mechanics.

This report presented a method to relate the discrete kinetic and kinematic quantities of the fundamental scale to their counterparts at the continuum scale. The relationship between discrete quantities and continuum quantities is developed using two simple concepts. The simple concepts of kinematics for the discrete entities are tied to continuum quantities using affine projections and the thermodynamic conjugates. The continuum quantities such as force and displacement are equated to their continuum counterparts, stress and strain, using the method of virtual power. The kinematics at the fundamental scale include the rotations of the discrete elements, which in contrast to those of material points in a continuum are independent of the translational motion. To accommodate the rotations as independent variables, the Cosserat continuum theory is used.

To demonstrate the usefulness of the Fortran algorithm and to provide insight into granular level engineering behavior, three test cases were examined. The test cases were used to compute the wall stress and REV strains and stresses that occur at the particle-scale. The results showed there was a disparity between the walls and REV stress determinations for the spherical sample volumes. In view of the inhomogeneity of contact forces, it could be argued that the extracted stresses are more representative of the stress state. Future testing of the algorithm should be applied to situations that are not dominated by the rigid boundaries.

References

Alonso-Marroquín, F. 2011. Static equations of the Cosserat continuum derived from intragranular stresses. *Granular Matter* 13(3):189-196.

Bardet, J. P., and I. Vardoulakis. 2001. The asymmetry of stress in granular media. *International Journal of Solids and Structures* 38(2):353-367.

Cosserat, E., and F. Cosserat. 1909. Theory of deformable body [in French]. Paris: Hermann.

Mindlin, R. D., and H. F. Tiersten. 1962. Effects of couple-stresses in linear elasticity. *Archive for Rational Mechanics and Analysis* 11(1):415-448.

Mühlhaus, H. B., and I. Vardoulakis. 1987. The thickness of shear bands in granular materials. *Geotechnique* 37(3):271-283.

Peters, J. F., and L. E. Walizer. 2013. Patterned nonaffine motion in granular media. *Journal of Engineering Mechanics* 139(10):1479-1490.

Peters, J. F. 2005. Some fundamental aspects of the continumization problem in granular material. *Journal of Engineering Mathematics* 52(1):231-250.

Sulem, J., and I. G. Vardoulakis. 2004. *Bifurcation analysis in geomechanics*. Boca Raton, FL: CRC Press.

Walsh, S. D., A. Tordesillas, and J. F. Peters. 2007. Development of micromechanical models for granular media. *Granular Matter* 9(5):337-352.

REPORT DOCUMENTATION PAGE

Form Approved
OMB No. 0704-0188

1. REPORT DATE *(DD-MM-YYYY)*	2. REPORT TYPE	3. DATES COVERED *(From - To)*
April 2019	Report 3	

4. TITLE AND SUBTITLE

Development of the Particle-Scale Definition of Stress and Strain for the Discrete Element Method

5a. CONTRACT NUMBER

5b. GRANT NUMBER

5c. PROGRAM ELEMENT NUMBER

6. AUTHOR(S)

W. D. Hodo, J. F. Peters, L. E. Walizer, D. P. McInnis,
and A. R. Carrillo

5d. PROJECT NUMBER

5e. TASK NUMBER

5f. WORK UNIT NUMBER
PM001 and MR001

7. PERFORMING ORGANIZATION NAME(S) AND ADDRESS(ES)

Geotechnical and Structures Laboratory
U.S. Army Engineer Research and Development Center
3909 Halls Ferry Road
Vicksburg, MS 39180-6199

8. PERFORMING ORGANIZATION REPORT NUMBER

ERDC TR-14-6; Report 3

9. SPONSORING / MONITORING AGENCY NAME(S) AND ADDRESS(ES)

U.S. Army Corps of Engineers
Washington, DC 20314-1000

10. SPONSOR/MONITOR'S ACRONYM(S)

USACE

11. SPONSOR/MONITOR'S REPORT NUMBER(S)

12. DISTRIBUTION / AVAILABILITY STATEMENT

Approved for public release; distribution is unlimited.

13. SUPPLEMENTARY NOTES

14. ABSTRACT

The discrete element method (DEM) provides a realistic approach to modeling materials at fundamental length scales. Materials at the discrete scale can be the particle size in granular materials, micrometer sizes when dealing with polycrystalline materials, or nanometer sizes when dealing with biologic materials. Complex material behavior can be simulated as relatively simple interactions between discrete entities, obviating the need for sophisticated constitutive models. The ultimate goal is to obtain the engineering behavior at the prototype scale at which problems are formulated in terms of continuum mechanics.

The simple concepts of kinematics for the discrete entities are tied to continuum quantities using affine projections and thermodynamic conjugates. The continuum quantities such as force and displacement are equated to their continuum counterparts, stress and strain, using the method of virtual power. The kinematics at the fundamental scale include the rotations of the discrete elements, which in contrast to those of material points in a continuum are independent of the translational motion. To accommodate the rotations as independent variables, the Cosserat continuum theory is used.
The procedures are implemented in a Fortran subroutine, which can be used in the post-processing phase of DEM simulations. Example computations for three test cases are included.

15. SUBJECT TERMS

Discrete particle physics
Micro-mechanical behavior
Discrete element method (DEM)
Nano-scale mechanics
Granular media
Materials – Mathematical models
Strains and stresses
Discrete element method

16. SECURITY CLASSIFICATION OF:			17. LIMITATION OF ABSTRACT	18. NUMBER OF PAGES	19a. NAME OF RESPONSIBLE PERSON
a. REPORT	b. ABSTRACT	c. THIS PAGE			19b. TELEPHONE NUMBER *(include area code)*
Unclassified	Unclassified	Unclassified		47	